GLOBAL JOURNAL OF PURE AND APPLIED SCIENCES VOL 16, NO. 4 2010: 469- 477
COPYRIGHT© BACHUDO SCIENCE CO. LTD PRINTED IN NIGERIA. ISSN 1118-0579
www.globaljournalseries.com; Email: info@globaljournalseries.com

A 3D MODEL FOR THICKNESS AND DIFFUSION CAPACITANCE OF EMITTER-BASE JUNCTION IN A BIFACIAL POLYCRYSTALLINE SOLAR CELL

S. MBODJI, B. MBOW, F. I. BARRO AND G. SISSOKO

(Received 1 December 2009; Revision Accepted 6, August 2010)

ABSTRACT

Through this paper, we present n^+-p-p^+ solar cell. Mathematical relations describing the generated carriers' density are expressed, using among others a new approach involving both junction and back surface recombination velocities in a 3D modelling study.

Based on the normalized carriers' density versus the base depth and operating an open circuit voltage, we study the space-charge layer thickness (Z) versus various parameters such as the grain size (g) and the grain boundaries recombination velocity (Sgb). Hence, the relationship between Z and the diffusion capacitance show that junction in the n^+-p-p^+ solar cell, when the columnar orientation is considered, is characterized by the plane capacitor properties.

PACS: 73.50.Pz

KEY WORDS: Polycrystalline Solar Cell, Grain Size and Grain Boundary, Capacitance, Junction

INTRODUCTION

The characterization of the space charge layer was first developed by Shockley in 1949 (Shockley, 1949). As Chockley's method is accurate for reverse and zero bias only, others researches(Liou and al., 1988, pp1571-34), (Chawla and al., 1971), (Liou and al.,1988, pp.1249-1253), taking in account of free carriers in space-charge layer of the p/n junction, developed a model for the space-charge layer thickness and the capacitance for all voltage and improved this method.

In high-frequency C-V characteristic (Rabbani and al., 1981, pp.661-664), (Jakubowski and al., 1981, pp.985-987) of both MIS and MOS capacitor, the Fermi potential, the substrate doping and the bulk generation lifetime in semiconductors can be determined. Exploiting the phase-sensitive LBIS analysis (Pernau and al.,2002, pp.442-445) authors show that the phase shift introduced by the solar cell depends on carriers lifetime, carriers diffusion velocity time decay and impedance incorporated in the solar cell itself. The capacitance method is also a useful procedure for the determination of the diffusion length in the Se-CdO photovoltaic cells (Champness and al., 1991 pp538-542.) Using a new approach involving both the junction recombination velocity ($SFu_{)\ and}$ the back surface recombination velocity ($Sbu_{)}$ in a 3D model study of a polycrystalline silicon bifacial solar cell (Diallo and al., 2008, pp 2003-211), we study the space-charge layer thickness and the capacitance. Within the first section basic theory is presented while the results related to the influence of grain size (g), grain boundary recombination velocity (Sgb) and wavelength (λ) are presented along the second part of this paper.

Theory

As an n^+-p-p^+ polycrystalline solar cell is made up by many small individual grains, grain boundary effects are important: among others grain boundaries act as electron-hole traps.

Regarding the physical process simulation, we can consider the fibrously oriented columnar grain as shown below in figure1 in a 3D while in the figure 2, the bifacial solar cell is in a planar configuration.

S. Mbodji, Laboratoire des Semi-conducteurs et d'Energie Solaire, Département de Physique, Faculté des Sciences et Techniques, Université Cheikh Anta Diop, Dakar, Senegal
B. Mbow, Laboratoire des Semi-conducteurs et d'Energie Solaire, Département de Physique, Faculté des Sciences et Techniques, Université Cheikh Anta Diop, Dakar, Senegal
F. I. Barro, Laboratoire des Semi-conducteurs et d'Energie Solaire, Département de Physique, Faculté des Sciences et Techniques, Université Cheikh Anta Diop, Dakar, Senegal
G. Sissoko, Laboratoire des Semi-conducteurs et d'Energie Solaire, Département de Physique, Faculté des Sciences et Techniques, Université Cheikh Anta Diop, Dakar, Senegal

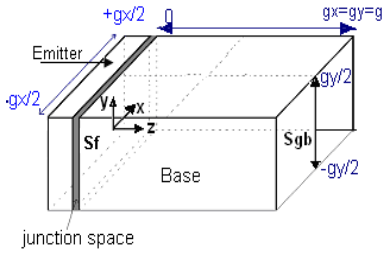

Figure 1: Isolated grain

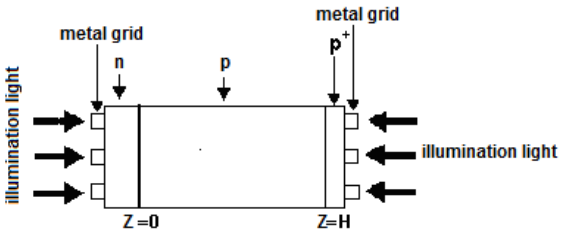

Figure 2: bifacial solar cell.

Using this isolated grain (figure 1), we made calculation to studying the variation of the main parameters, for instance: grain size (g), grain boundaries recombination velocity(Sgb) and wavelength(λ).
Studying the influence of the grain size and the excess minority carriers density, some authors (Diallo and al., 2008, pp 2003-211), showed that the number of excess minority carriers increases and decreases respectively with the grain size(g) and the grain boundary recombination velocity(Sgb); they (Diallo and al., 2008, pp 2003-211), also proved that central areas of each grain, contrary to the corner, aren't affected by the recombination occurring at the interfaces' level.
Theses two parameters (g; Sgb) influence the photocurrent (Iph) and the photo-voltage (Uph) (Diallo and al., 2008, pp 2003-211). In fact both Iph and Uph decrease when the grain size decreases and increase when the grain boundary recombination velocity increases.

Considering the emitter as a dead (non active) area, the excess minority carrier distribution in the base, seen as a greater contribution to the photo-conversion, is derived from solving the continuity' equation:

$$D\cdot\left(\frac{\partial^2\delta_u(x,y,z)}{\partial^2 x}+\frac{\partial^2\delta_u(x,y,z)}{\partial^2 y}+\frac{\partial^2\delta_u(x,y,z)}{\partial^2 z}\right)-\frac{\delta_u(x,y,z)}{\tau}=-G_u(z) \quad (1)$$

where D is excess minority carriers diffusion constant while L is the diffusion length.
The following three cases of illumination have been considered: the front illumination, the rear side illumination and the simultaneous illumination. The electron-hole pairs generation rate is expressed as follows (Sissoko and al., 1998, pp.1856-1859).

$$G_u(z)=\alpha\cdot I_0\cdot(1-R)\cdot\left(\varepsilon\cdot\exp(-\alpha\cdot z)+\gamma\cdot\exp(-\alpha\cdot(H-z))\right) \quad (2)$$

The subscript u indicates how the solar cell is illuminated: front side u=fr (ε=1 and γ=0), rear side u=re (ε=0 and γ=1) or simultaneous illumination u=d (ε=1 and γ=1).
α is the absorption coefficient of light for a wavelength λ , I_0 is the incident photon flux (Green and al., 1995, p.189-92)
The general solution of the continuity equation (Equation 1) is given as (DUGAS, 1994, pp.71-88).

$$\delta_u(x,y,z)=\sum_k^{\infty}\sum_j^{\infty}Z_{kj}(z)\cdot\cos(x\cdot c_k)\cdot\cos(y\cdot c_j) \quad (3)$$

The factors c_k and c_j are eigen values and depend on grain size and grain boundaries' recombination velocity only.
Inserting the (Equation 3) into (Equation 1) and replacing the expression generation by its value and taking into account of the fact that $\cos(c_k x)$ and $\cos(c_j x)$ are orthogonal functions, we obtain a general expression for $Z_{kj}(z)$.This expression contains two constants derived using interfaces' boundary conditions while the factors c_k and c_j in (Equation 3) are determined using the grain boundaries'condtions.
The boundary conditions at the n^+-p interface (z=0) are:

$$D\cdot\left.\frac{\partial\delta_u(x,y,z)}{\partial z}\right|_{z=0}=SF_u\cdot\delta_u(x,y,z=0) \quad (8)$$

SF_u is the junction recombination velocity (Diallo and al., 2008, pp 2003-211) and represents the sum of two terms: $SF_u=Sf0_u+Sf_j$. Sf_j is the external load related to the current flow and j defines the operating point of the cell (Diallo and al., 2008, pp 2003-211). $Sf0_u$ is defined as the intrinsic junction recombination velocity related to the

shunt resistance, an internal load of the solar cell due to losses at the junction level. For each illumination mode, the intrinsic junction recombination velocity is calculated through the derivation of the photocurrent.
Therefore the expression of $Sf0_u$ varies depending on illumination scenario (Diallo and al., 2008, pp 2003-211).
At the back side of the bifacial solar cell, we use the boundary condition for z=H:

$$D \cdot \left. \frac{\partial Z_{kj}(z)}{\partial z} \right|_{z=H} = -Sb_u \cdot Z_{kj,u}(H) \tag{9}$$

Sb_u is the back surface recombination velocity. It quantifies the rate at which excess minority carriers are lost at the back surface of the cell (Diallo and al., 2008, pp 2003-211).The derivation of the photocurrent, associated to SF_u, provides for different illumination modes the expression of Sb_u.
A contact level of two grains in the direction (Ox) and (Oy), boundary conditions are:

$$D \cdot \left. \frac{\partial \delta(x,y,z)}{\partial x} \right|_{x=\pm\frac{g}{2}} = \mp Sgb \cdot \delta_u(\pm\frac{g}{2}, y, z) \tag{10}$$

And

$$D \cdot \left. \frac{\partial \delta(x,y,z)}{\partial x} \right|_{y=\pm\frac{g}{2}} = \mp Sgb \cdot \delta_u(x, \mp\frac{g}{2}, z) \tag{11}$$

The resolution of above two equations gives transcended equations allowing the determination of the factors ck and cj.
The capacitance of the solar cell is presented as follows:

$$C_u(z,g,Sgb,SF_u,Sb_u,\lambda) = \frac{q}{V_T} \cdot \left[\delta_u(z,g,Sgb,SF_u,Sb_u,\lambda) + m_0\right] \tag{12}$$

q is the elementary electron charge, V_T is the thermal voltage and $m_0 = \frac{n_i^2}{Nb}$ with Nb the base doping density and n_i intrinsic carriers density.

RESULTS AND DISCUSSIONS

3.1 Normalized carriers' density versus base depth for different values of SF_u

We have in figures 3, 4 and 5 the curves of normalized carriers density versus base depth when the solar cell is in its open circuit voltage (Sf_j=0) or short circuit photocurrent mode ($SF_{av}\rightarrow\infty$). Figure.3 represents the normalized carriers density when $0 < z < 0.005cm$ for the front side illumination mode. For rear side and simultaneous illumination modes we have figure 4 and 5 with the open circuit and short circuit operating points.

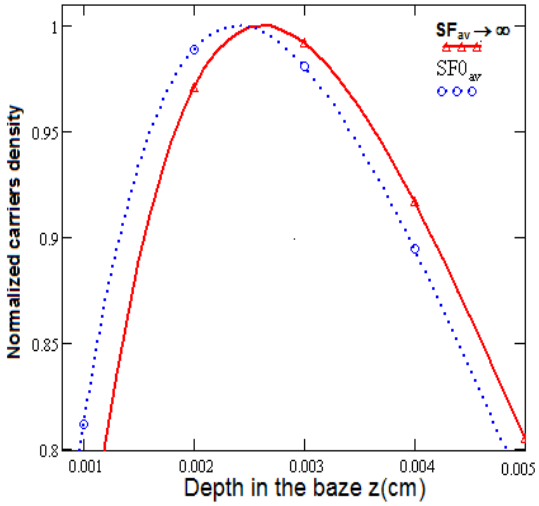

Figure.3: Normalized carriers density versus base depth when the solar cell is illuminated by front side.

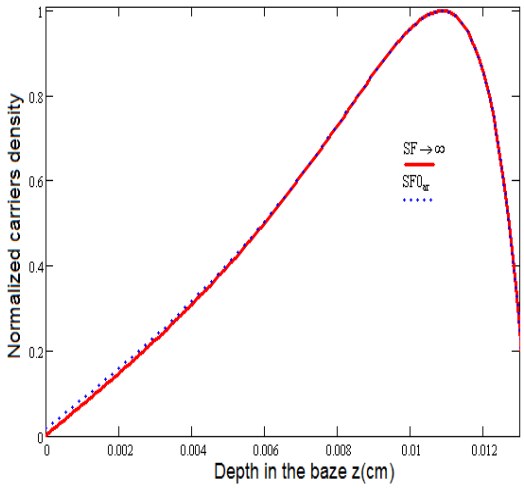

Figure.4: Normalized carriers density versus base depth for the rear side illumination mode of the solar cell.

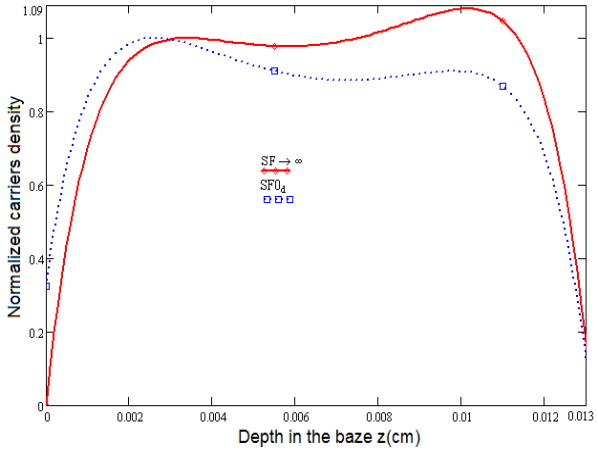

Figure.5: Normalized carriers density versus base depth when the solar cell is simultaneously illuminated both front and rear sides

We find different characteristics' regions when solar cell is illuminated:

For the front side illumination, curves of open and short circuit exhibit two regions in the base depth. The first region closed to the junction with a positive slope which increases as SF_{av} is higher and corresponds to minority carriers collection region. This is an additive space-charge region $Z_{0,av}$ to initial diffusion depletion layer. We find also the extension of this region width with the increasing of the junction recombination velocity SF_{av}.

When the solar is illuminated by the rear side contrary to the front side, the maxima points of the excess minority carriers density are in the back side of the solar cell and are independent of the operating point. Like the front side, we have two regions: the first region corresponds to carriers recombined in the bulk and those collected at the junction. The second region refers to carriers which are lost at the back surface of the photovoltaic solar cell.

The double sided illumination mode gives three regions. The collection region is the first region closed to the junction, the second and third region correspond respectively of the recombination in the bulk and the back of the solar cell.

As the junction depth varies only for front and simultaneous illumination modes (for the rear side illumination, the variation is neglected), we determine extension region width $Z_{0,u}$. Hence we calculate for different values of junction recombination velocity the photovoltage, the excess minority carries density and the capacitance corresponding to different values $Z_{0,u}$.

The following figures 6 and 7 are the plots for inverse capacitance $C_{0,u}^{-1}$ versus space-charge layer extension $Z_{0,u}$ when the bifacial solar cell is illuminated respectively in case of front side mode and simultaneously both front and rear sides.

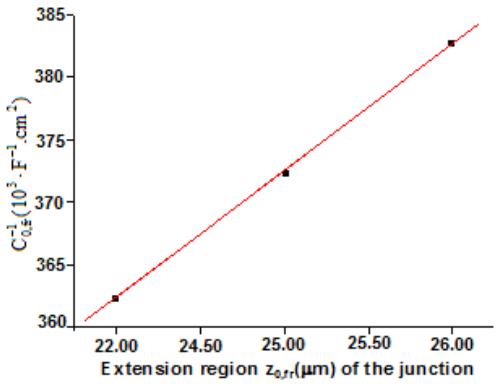

Figure.6: $C_{0,fr}^{-1}$ versus space-charge layer extension thickness.

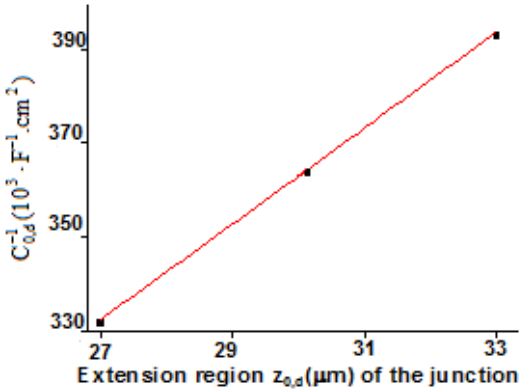

Figure.7: $C_{0,fr}^{-1}$ versus space-charge layer extension thickness.

The inverse capacitance versus extension region is a straight line. As shown by some authors (Sissoko and al., 1998, pp1852-1855) for the single crystal, when grain size, junction recombination velocity and wavelength are fixed values, the diffusion capacitance resulting from contribution of the free charge carriers for a solar cell in real operating point can be considered as a plane capacitor.

3.2 Extension region width for each grain size (g), grain boundaries recombination velocity (Sgb) and wavelength (λ).

As we above proved that diffusion capacitance in real operating of the solar cells is a plane capacitance, we assume that free carriers at the junction are responsible of efficiency in semiconductors devices. Hence, we use the figure 8 to draw an equivalent circuit where the capacitance ($Z_{0,u}$) represent the solar cell in series with the load charge.

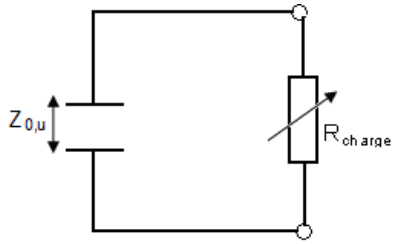

Figure.8: Equivalent circuit of an ideal photovoltaic cell with an externally applied load.

We conclude also that the capacitance C_u associated to the whole minority carriers collection layer is reduced to the Shockley's model (Shockley, 1949) when the photovoltage is constant.

Using one normalized carrier density versus base depth for one grain size, we determine the constant photovoltage $\mathbf{V_u(z_{0,u}, g, Sgb, SF, Sb, \lambda)}$.

With such a fixed value of voltage, we solved the following (Equation 13) for each grain size, grain boundaries' recombination velocity and wavelength; then the corresponding extension region $Z_{0,u}$ is obtained when other parameters are fixed.

$$\mathbf{V_u(z,g,Sgb,SF,Sb,\lambda) = V_u(z_0,g,Sgb,SF,Sb,\lambda)} \quad (13)$$

Solar capacitance in open circuit voltage is then calculated using values of $Z_{0,u}$ through the relation:

$$\mathbf{C_{0,u} = \frac{\varepsilon \cdot S}{Z_{0,u}}} \quad (14)$$

where S=1cm^2 and the dielectric constant $\boldsymbol{\varepsilon = \varepsilon_0 \cdot \varepsilon_r = 12 \cdot 8.85 \cdot 10^{12}\ F.cm^{-1}}$.

In fact $\boldsymbol{\varepsilon_r = 12}$ is the relative dielectric constant of the semiconductor and $\boldsymbol{\varepsilon_0 = 8.85 \cdot 10^{12}\ F \cdot cm^{-1}}$ is the permittivity for the vacuum.

Results are presented below in tables 1 to 4 for the front size and both front side and rear side illumination modes.

Table.1: Values of characteristic parameters of the junction when g varies and the solar cell is illuminated in case of front side mode.

g (μm)	$Z_{0,fr}$ (μm)	V_{fr} ($Z_{0,fr}$)	$E_{ZCE,fr}$ (V.m^{-1})	$C_{0,fr}$ (nF.cm^{-2})	δ_{fr} $(10^{11} \cdot cm^{-3})$
20	25,12	0.57 V	22691	42.27	1.50
23	18,56	0.57 V	30711	57.21	2.03
26	16,49	0.57 V	34566	64.40	2.29
29	15,18	0.57 V	37549	69.96	2.49
32	14,22	0.57 V	40084	74.68	2.66
35	13,46	0.57 V	42347	78.90	2.81
38	12,84	0.57 V	44392	82.71	2.94
41	12,32	0.57 V	46266	86.20	3.07
44	11,86	0.57 V	48060	89.54	3.19

Table.2: Values of characteristic parameters of the junction when g varies and the solar cell is illuminated in case of both front and rear side mode.

g (μm)	$Z_{0,d}$ (μm)	V_d ($Z_{0,d}$)	$E_{ZCE,d}$ (V.m^{-1})	$C_{0,d}$ (nF.cm^{-2})	δ_d $(10^{11} \cdot cm^{-3})$
32	21.55	0.57V	17225	49.28	1.14
35	18.65	0.57V	26450	56.94	1.75
38	16.87	0.57V	30563	62.95	2.02
41	15.61	0.57V	33787	68.03	2.24
47	14.63	0.57V	36515	72.59	2.42
50	13.83	0.57V	38961	76.78	2.58
53	12.57	0.57V	41214	84.48	2.73
56	12.03	0.57V	45346	88.13	3.00

Table.3: Values of characteristic parameters of the junction when Sgb varies and the solar cell is in the mode of illuminated front side.

Sgb ($cm.s^{-1}$)	$Z_{0,fr}$ (μm)	V_{fr} ($Z_{0,fr}$)	$E_{ZCE,fr}$ ($V.m^{-1}$)	$C_{0,fr}$ ($nF.cm^{-2}$)	δ_{fr} $(10^{11} \cdot cm^{-3})$
158	10.80	0.57 V	52777	98,33	3.50
200	11.13	0.57 V	51212	95,41	3.39
251	11.55	0.57 V	49350	91,94	3.27
316	12.10	0.57 V	47107	87,76	3.12
398	12.82	0.57 V	44461	82,83	2.95
501	13.80	0.57 V	41304	76,95	2.74
630	15.22	0.57 V	37450	69,77	2.48
794	17.51	0.57 V	32552	60,65	2.16
1000	25.42	0.57 V	22423	41,77	1.48

Table.4: Values of characteristic parameters of the junction when Sgb varies and the solar cell is illuminated in both front and rear side.

Sgb ($cm.s^{-1}$)	$Z_{0,d}$ (μm)	V_d (Volt)	$E_{ZCE,d}$ ($V.m^{-1}$)	C_d ($nF.cm^{-2}$)	δ_d $(10^{11} \cdot cm^{-3})$
158	10.93	0.57	51150	97.16	3.46
200	11.35	0.57	50220	93.58	3.33
251	11.89	0.57	47939	89.31	3.18
316	12.59	0.57	45274	84.35	3.00
398	13.53	0.57	42128	78.49	2.79
501	14.83	0.57	38435	71.61	2.55
630	16.72	0.57	34090	63.51	2.26
794	19.91	0.57	28628	53.34	1.90
1000	33.09	0.57	17225	32.09	1.14

The solar cell's diffusion capacitance increases with the grain size and decreases with the grain boundaries recombination velocity or the wavelength. Compared to such a behavior of the capacitance, instead the variation of the space charge layer is not affecting the voltage: while the junction width is increasing or deceasing, the photovoltage is constant.

For the junction's solar cell in illumination the resulting electric field $E_{ZCE,u}$ ($E_{ZCE,u} = \frac{V_u}{Z_{0,u}}$) is different from the intrinsic electric field E_0 of any p-n junction: it increases with the grain size ,and when the grain boundary recombination velocity or the wavelength increases, the electric field decreases.

In figures 9 to 12, we present inverse diffusion capacitance with extension region of the junction for the front and the simultaneous illumination modes. In Figures 9 and 10 grain size is varying. The effect of grain boundary recombination velocity when the grain size and the wavelength are fixed values is shown in figures 11 and 12.

Analysing these figures, we note that inverse diffusion capacitance $C_{0,u}^{-1}$ with extension region of the junction $Z_{0,u}$ is a straight line as shown by other authors (Sissoko and al., 1998, pp1852-1855).The junction of the solar is then considered as a plane capacitor.

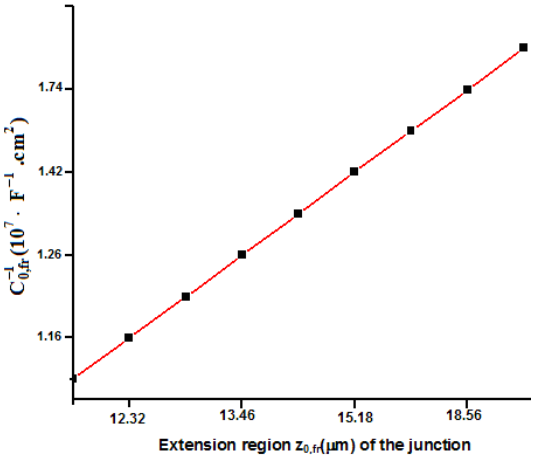

Figure .9: $C_{0,fr}^{-1}$ front side illumination mode versus space-charge layer extension thickness;

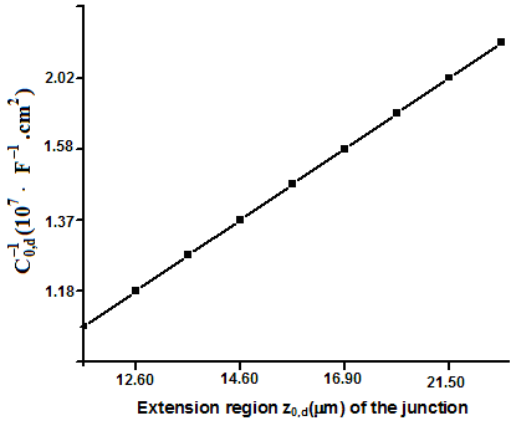

Figure.10: $C_{0,d}^{-1}$ double side illumination versus space charge layer extension thickness $Z_{0,d}$

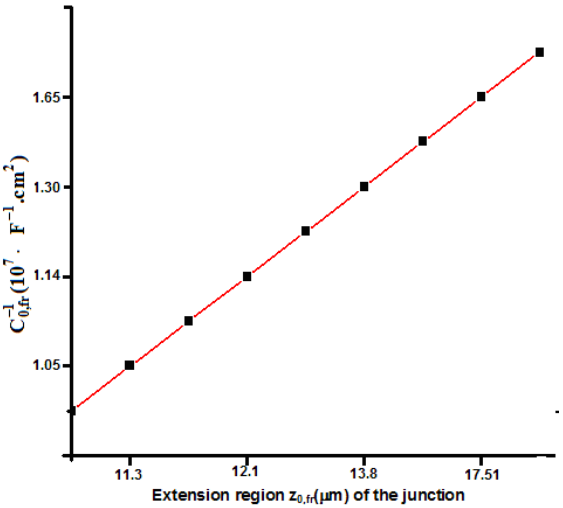

Figure.11: $C_{0,fr}^{-1}$ front side illumination mode versus space-charge layer extension thickness;

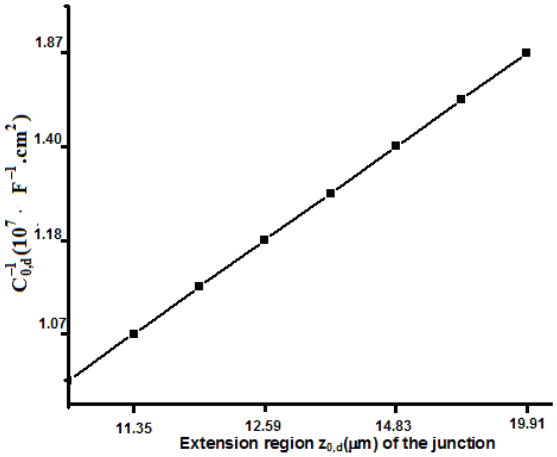

Figure.12: $C_{0,d}^{-1}$ double side illumination versus space charge layer extension thickness $Z_{0,d}$

CONCLUTION

Based on the behavior of normalized minority carriers' density versus the base depth of a solar cell under different illumination modes, the inverse of solar cell's diffusion capacitance and the extension layer thickness of the junction were simulated and the minority carriers' collection layer can be finally considered as plane capacitor in case of columnar orientation .

The effects of junction recombination velocity, illumination modes, wavelength, grain size and grain boundaries recombination velocity on the diffusion capacitance were shown. For instance the diffusion capacitance increases with grain size (g) and decreases when grain boundary recombination velocity (Sgb) increases.

REFERENCES

Shockley, W., 1999. Bell Syst. Techn. J. 28, 435.

Liou, J. J., Lindholm, F. A., and Park, J. S., 1988. IEEE Trans Electronic Devices ED.34, p.1571

Chawla, B. R. and Gummel, H. K., 1971. IEEE Trans Electron Devices. Ed-18, pp.178

Liou, J. J and Lindholm, F. A., 1988. J. Appl Phys.64 (3), pp.1249-1253

Rabbani, K. S and Lamb, D. R., 1981. Solid State Electronic, Vol.24, pp.661-664

Jakubowski, A., Solid State Electronic, 1981, Vol. 24, No.10, pp.985-987

Pernau, Th., Fath, P., and Bucher, E., 2002. Conference record of the twenty-ninth IEEE photovoltaic specialists conference, pp.442-445

Champness, C. H., Shukri , Z. A and Chan, C. H.,1991. Can.J.Phys.69, pp538-542.

Diallo, H. L., Maiga, A. S., Wereme, A and Sissoko, G., 2008, Eur.Phys.J.Appl.Phys.42, 2003-211.

Sissoko, G. Correa, A., Nanema, E., Diarra, M. N., Ndiaye A. L and Adj, A., World Renewable Energy Congress, 1998, pp.1856-1859.

Green, M. A. and Keevers, M., 1995. Progress in Photovoltaics, vol.3, no.3. P.189-192

DUGAS, J., 1994. Solar Energy Materials and Solar Cells, 32 pp.71-88,.

SISSOKO, G., DIENG, B., CORREA, A., ADJ, M and D. AZILINON, 1998. Proceedings of the World Renewable Energy Congress, pp1852-1855